Environmental Science & Technology

Article

pubs.acs.org/est

Production of Nitrous Oxide from Nitrite in Stable Type II Methanotrophic Enrichments

Jaewook Myung,[†] Zhiyue Wang,[†] Tong Yuan,[‡] Ping Zhang,[‡] Joy D. Van Nostrand,[‡] Jizhong Zhou,[‡] and Craig S. Criddle*[,†,§,∥]

[†]Department of Civil and Environmental Engineering, Stanford University, Stanford, California 94305, United States

[‡]Institute for Environmental Genomics, Department of Microbiology and Plant Science, University of Oklahoma, Norman, Oklahoma 73019, United States

[§]Woods Institute for the Environment, Stanford, California 94305, United States

[∥]William and Cloy Codiga Resource Recovery Center, Stanford, California 94305, United States

Supporting Information

ABSTRACT: The coupled aerobic−anoxic nitrous decomposition operation is a new process for wastewater treatment that removes nitrogen from wastewater and recovers energy from the nitrogen in three steps: (1) NH_4^+ oxidation to NO_2^-, (2) NO_2^- reduction to N_2O, and (3) N_2O conversion to N_2 with energy production. Here, we demonstrate that type II methanotrophic enrichments can mediate step two by coupling oxidation of poly(3-hydroxybutyrate) (P3HB) to NO_2^- reduction. Enrichments grown with NH_4^+ and NO_2^- were subject to alternating 48-h aerobic and anoxic periods, in which CH_4 and NO_2^- were added together in a "coupled" mode of operation or separately in a "decoupled mode". Community structure was stable in both modes and dominated by *Methylocystis*. In the coupled mode, production of P3HB and N_2O was low. In the decoupled mode, significant P3HB was produced, and oxidation of P3HB drove reduction of NO_2^- to N_2O with ∼70% conversion for >30 cycles (120 d). In batch tests of wasted cells from the decoupled mode, N_2O production rates increased at low O_2 or high NO_2^- levels. The results are significant for the development of engineered processes that remove nitrogen from wastewater and for understanding of conditions that favor environmental production of N_2O.

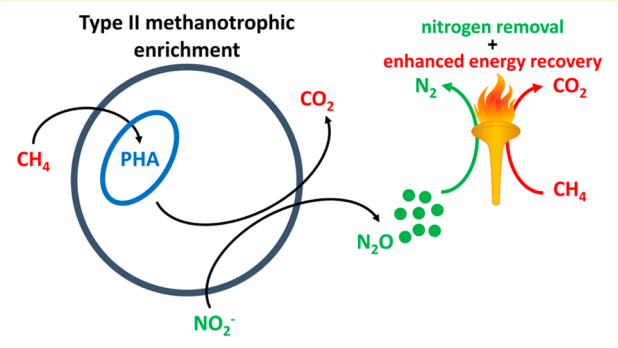

INTRODUCTION

Methanotrophic (methane-oxidizing) bacteria largely use methane (CH_4) as their sole source of energy and carbon, oxidizing it in the marine environment, wetlands, sediments, soils, and landfills.[1] In addition to their role in the carbon cycle, methanotrophs play an important role in the nitrogen cycle.[2−10] Both methanotrophs and ammonia-oxidizing bacteria possess monooxygenase enzymes that can oxidize CH_4 to methanol or ammonium (NH_4^+) to hydroxylamine.[11,12] The hydroxylamine can then be oxidized to nitrite (NO_2^-) and reduced to nitrous oxide (N_2O).[13,14] Typically, N_2O is viewed as an unwanted byproduct of wastewater treatment. Like CH_4, N_2O is a significant greenhouse gas included in the Kyoto Protocol, with a global warming potential 180 times that of carbon dioxide (CO_2),[15] but it is also a source of renewable energy. It is well-known for its use as a "power booster" when used as a hydrocarbon co-oxidant in race cars,[16,17] and it can increase energy production at wastewater treatment plants when used as a biogas CH_4 co-oxidant.[18] When CH_4 is oxidized by O_2, the enthalpy of combustion, ΔH_c^0, is −890 kJ mol^{-1}; when N_2O is the oxidant, ΔH_c^0, is −1219 kJ mol^{-1}, a 37% increase.

Recently, Scherson et al.[18,19] introduced the coupled aerobic−anoxic nitrous decomposition operation (CANDO), a process in which NO_2^- is converted biologically to N_2O and the N_2O is recovered for use as a biogas oxidant. The process requires two steps: in step one, ammonia-oxidizing microorganisms oxidize NH_4^+ to NO_2^-; in step two, heterotrophic bacteria oxidize intracellular poly(3-hydroxybutyrate) (P3HB) and simultaneously reduce NO_2^- to N_2O. The intracellular P3HB is generated from volatile fatty acid fermentation products. In this study, we demonstrate that type II methanotrophs can generate P3HB from CH_4 feedstock and efficiently couple its oxidation to the reduction of NO_2^- to N_2O (step 2 of the CANDO process).

Received: July 13, 2015
Revised: August 20, 2015
Accepted: August 21, 2015
Published: August 24, 2015

DOI: 10.1021/acs.est.5b03385
Environ. Sci. Technol. 2015, 49, 10969−10975

MATERIALS AND METHODS

Culture Conditions. Unless otherwise specified, all cultures were grown in medium JM2. Medium JM2 contained the following chemicals per liter of solution: 2.4 mM $MgSO_4 \cdot 7H_2O$, 0.26 mM $CaCl_2$, 36 mM $NaHCO_3$, 4.8 mM KH_2PO_4, 6.8 mM K_2HPO_4, 10.5 μM $Na_2MoO_4 \cdot 2H_2O$, 7 μM $CuSO_4 \cdot 5H_2O$, 200 μM Fe-EDTA, 530 μM Ca-EDTA, 5 mL of trace metal solution, and 20 mL of vitamin solution. The trace stock solution contained the following chemicals per liter of solution: 500 mg of $FeSO_4 \cdot 7H_2O$, 400 mg of $ZnSO_4 \cdot 7H_2O$, 20 mg of $MnCl_2 \cdot 7H_2O$, 50 mg of $CoCl_2 \cdot 6H_2O$, 10 mg of $NiCl_2 \cdot 6H_2O$, 15 mg of H_3BO_3, 250 mg of EDTA. The vitamin stock solution contained the following chemicals per liter of solution: 2.0 mg of biotin, 2.0 mg of folic acid, 5.0 mg of thiamine·HCl, 5.0 mg of calcium pantothenate, 0.1 mg of vitamin B12, 5.0 mg of riboflavin, and 5.0 mg of nicotinamide.

All cultures were incubated in 25 mL of serum bottles (Wheaton, Mealville, NJ, USA) capped with butyl-rubber stoppers and crimp-sealed under 1:1.5 CH_4/O_2 headspace. All bottles were incubated horizontally on orbital shaker tables at 150 rpm. The incubation temperature was 30 °C.

Nitrite- and Ammonium-Fed Methanotrophic Enrichment Cultures. Fresh activated sludge was obtained from the aeration basin at the Palo Alto Regional Water Quality Control Plant (community structure in Table S1, Palo Alto, CA, USA). Large material was removed by filtering through a 100-μm cell strainer (BD Falcon Biosciences, Lexington, TN, USA). The dispersed cells were centrifuged (10000*g*) for 5 min to create a pellet. The pellet was resuspended in medium JM2 and shaken to obtain a dispersed cell suspension. Aliquots (15 mL) of the suspension were transferred to two 250 mL serum vials containing 35 mL of medium JM2. Every 24 h for 25 d, the headspace of each bottle was flushed with a CH_4/O_2 mixture (molar ratio of 1:1.5). For the first 7 days, each bottle received 0.4 mL of an NH_4^+ stock solution (1.35 M ammonium chloride) every 24 h. After the 8th day, 0.5 mL of a NO_2^- stock solution (0.2 M sodium nitrite) was also added. On the 26th day, the enrichments in both bottles were centrifuged (10000*g*) for 5 min, and the pellets were resuspended in 15 mL of medium JM2. These suspensions were divided into 5 mL aliquots for inoculation of three fed-batch serum bottle reactors (250 mL). Each fed-batch reactor initially contained 5 mL of inoculum, 44.1 mL of medium JM2, 0.4 mL of NH_4^+ stock, and 0.5 mL of NO_2^- stock (total volume 50 mL).

Coupled Mode vs Decoupled Mode. After a 25-d adaptation period, each of the three CH_4-fed enrichments was subject to alternating 48-h aerobic and 48-h anoxic periods in either a "coupled" mode or a "decoupled" mode (Figure S1): in the coupled mode, NH_4^+ and NO_2^- were supplied together before cell growth (t = 0 h); in the decoupled mode, NH_4^+ was supplied before cell growth, whereas NO_2^- was supplied after cell growth (t = 48 h). The total amount of NH_4^+ and NO_2^- added in a 96-h period was the same for each case.

In the coupled mode, triplicate enrichments in serum bottles containing 10 mL of carryover culture from the previous cycle were subject to the following repeating cycle every 96 h: (1) addition of 40 mL of fresh medium (39.3 mL of medium JM2, 0.2 mL of NH_4^+ stock, and 0.5 mL of NO_2^- stock); (2) flushing for 5 min with a CH_4/O_2 molar ratio of 1:1.5; (3) incubation for 48 h at 30 °C; (4) flushing for 5 min with helium gas to establish anoxic condition; and (5) incubation for a second 48-h period at 30 °C.

In the decoupled mode, triplicate enrichments in serum bottles containing 10 mL of carryover culture from the previous cycle was subject to the following repeating cycle every 96 h: (1) addition of 40 mL of fresh medium (39.8 mL of medium JM2, 0.2 mL of NH_4^+ stock); (2) flushing for 5 min with a CH_4/O_2 molar ratio of 1:1.5; (3) incubation for 48 h at 30 °C. (4) flushing for 5 min with helium gas to establish anoxic condition; (5) addition of 1.5 mL of NO_2^- stock after 48 h of incubation; and (6) incubation for a second 48-h period at 30 °C. In some decoupled cycles, the second 48-h period was modified to evaluate the effect of different levels of added O_2 (0−50% O_2 in headspace) and NO_2^- (0−200 mg of NO_2−N/L) on N_2O production.

Microbial Community Analysis. Genomic DNA was recovered from the activated sludge inoculum and from triplicate bioreactor samples taken at different time points. The DNA was purified, amplified by PCR, then sequenced using the MiSeq Illumina platform (Illumina, San Diego, CA, USA). Detailed protocols are described in the Supporting Information.

Analytical Methods. To analyze concentrations of CH_4, O_2, CO_2, N_2, and N_2O, 0.5 mL of gas phase from each reactor bottle was injected onto a GOW-MAC gas chromatograph with an Altech CTR 1 column and a thermal conductivity detector. The following method parameters were used: injector, 120 °C; column, 60 °C; detector, 120 °C; and current, 150 mV. Peak areas of CH_4, O_2, CO_2, N_2, and N_2O were compared with standards and quantified using the software ChromPerfect (Justice Laboratory Software, Denville, NJ, USA).

Inorganic nitrogen (NH_4^+, NO_3^-, and NO_2^-) concentrations were measured colorimetrically. Samples were centrifuged (10000*g*) for 5 min, and the supernatants were diluted 1:500 in Milli-Q water before colorometric analysis with a Westco Smartchem 200 discrete analyzer (Brookfield, CT, USA).

To analyze total suspended solids (TSS), 0.5−5.0 mL of cell suspension was filtered through prewashed, dried, and preweighed 0.2-μm membrane filters (Pall, Port Washington, NY, USA). After drying at 80 °C for 24 h, the dried filters and samples were weighed on an AD-6 autobalance (PerkinElmer, Norwalk, CT, USA).

Poly(3-hydroxybutyrate) (P3HB) Measurement. Between 5 and 10 mg of freeze-dried biomass was weighed then transferred to a 12 mL glass vial. Each vial was amended with 2 mL of methanol containing sulfuric acid (3%, vol/vol) and benzoic acid (0.25 mg/mL methanol), supplemented with 2 mL of chloroform, and sealed with a Teflon-lined plastic cap. All vials were shaken then heated at 95−100 °C for 3.5 h. After cooling to room temperature, 1 mL of deionized water was added to create an aqueous phase separated from the chloroform organic phase. The reaction cocktail was mixed on a vortex mixer for 30 s then allowed to partition until phase separation was complete. The organic phase was sampled by syringe and analyzed using a GC (Agilent 6890 N) equipped with an HP-5 column (containing 5% phenyl-methylpolysiloxane; Agilent Technologies, Palo Alto, CA, USA) and a flame ionization detector. DL-Hydroxybutyric acid sodium salt (Sigma-Aldrich, St Louis, MO, USA) was used to prepare external calibration curves. The P3HB content (wt %) of the samples was calculated by normalizing to initial dry mass.

Electron Microscopy. To verify the presence of intracellular P3HB granules in microbes and to compare the amount of P3HB granules at different times, microbial samples were fixed with 2% glutaraldehyde and 4% paraformaldehyde in 0.1

DOI: 10.1021/acs.est.5b03385
Environ. Sci. Technol. 2015, 49, 10969−10975

M sodium cacodylate buffer ($Na(CH_3)_2AsO_2 \cdot 3H_2O$), pH 7.4 for 48 h at 4 °C. To coat cells in gelatin, cells were washed in the buffer and resuspended in 10% warm gelatin for 5 min, placed on ice for 5 min, then cut into blocks and postfixed using cold osmium tetroxide (OsO_4). Postfixed samples were dehydrated using ethanol and acetonitrile, embedded in an epoxy resin mixture, then cut into ultrathin sections, which were then mounted on copper grids. The grids were observed with a JEOL TEM 1400 microscope equipped with a Gatan 967 slow-scan, cooled CCD camera. Images were processed using Digital Micrograph, Digital Montage, and TEM Auto tune.

Carbon, Nitrogen, and Electron Balances. We prepared carbon balance (C-moles), nitrogen balances (N-moles), and electron balances (e-moles) for each bottle using measured data for P3HB produced, CH_4 consumed, CO_2 generated, NH_4^+ consumed, NO_3^- consumed, NO_2^- consumed, N_2O generated, N_2 generated, and TSS, assuming the TSS is 90% volatile suspended solids (VSS) with an empirical formula of $C_5H_7O_2N$.[20] Electron balances were calculated relative to the reference oxidation states of CO_2 and O_2 for organic carbon and H_2O. All nitrogen species were calculated relative to the reference oxidation state of NO_3^-.

RESULTS

Community Analysis. After applying both coupled and decoupled cycling strategies to enrich for methanotrophic communities, we extracted genomic DNA from triplicate samples on cycles 13, 22, 29, and 39 (Figure 1). Microbial community structure in both the coupled and the decoupled cycling modes remained stable for 26 cycles of operation. *Methylocystis* dominated the reactors, followed by other minor genera including *Hyphomicrobium*, *Hydrotalea*, and *Terrimonas*. *Hyphomicrobium* are facultative methylotrophs that grow on C1 and C2 compounds, and some are known to accumulate intracellular P3HB.[21,22] *Hyphomicrobium* spp. that couple methanol oxidation to denitrification are well studied.[23,24] Little is known about the genera *Hydrotalea* and *Terrimonas*.

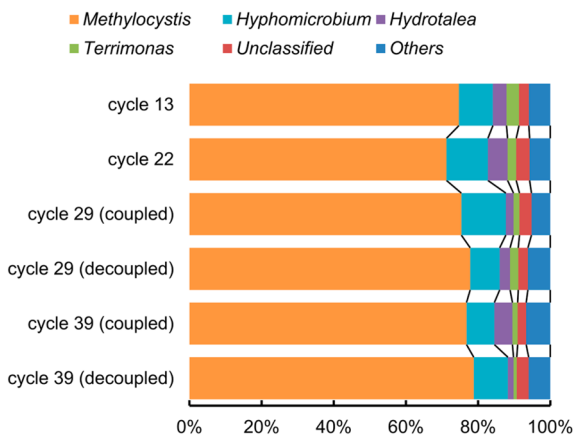

Figure 1. Genus-level microbial community structures for replicated bioreactors at four different time points. Triplicate samples were obtained for each time point. In cycles 29 and 39, coupled reactors and decoupled reactors were separately sampled and sequenced.

Comparison between the Coupled Mode and the Decoupled Mode. During a period of stable community structure (cycles 13−39), the initial and final concentrations of NH_4^+, NO_2^-, NO_3^-, P3HB, and TSS were monitored for both the coupled and decoupled modes of operation. Cycle-to-cycle results did not change appreciably, indicating both functional and community stability. For one 96-h cycle during this period (cycle 24), we monitored substrate utilization and product generation in detail. The results are summarized in Figure 2. The small error bars indicate a high degree of reproducibility.

In the coupled mode (Figure 2a), microbial growth was inhibited: only 28 ± 5% of the added NH_4^+ was consumed, and the maximum biomass concentration leveled off at 483 ± 105 mg of TSS L^{-1} (Table 1). Little P3HB was produced (<5%), and there was essentially no change in P3HB levels. NO_2^- removal efficiency was poor (8 ± 3%), as was the efficiency of conversion of NO_2^- to N_2O (6 ± 3%). The maximum specific rate of N_2O production was low (0.039 ± 0.009 mg of N_2O−N L^{-1} h^{-1}), as was total inorganic nitrogen removal efficiency (19 ± 5%).

By contrast, in the decoupled mode (Figure 2b), we observed three phases of microbial growth: phase 1, aerobic growth with cell division and nitrogen assimilation (24 h); phase 2, aerobic P3HB accumulation under nitrogen-limiting conditions (24 h); and phase 3, anoxic P3HB oxidation and coupled reduction of NO_2^- to nitrous oxide (48 h). In phase 1, CH_4 oxidation was rapid, more than 99% of the added NH_4^+ was assimilated, and biomass concentration increased to approximately 850 mg of TSS L^{-1}; in phase 2, reactive nitrogen was absent, CH_4 oxidized at a slower rate, P3HB accumulated (up to 40 ± 3 wt %), and biomass concentration increased to 1153 ± 72 mg of TSS L^{-1} (Table 1); and in phase 3, ∼10 wt % of the P3HB was oxidized, and NO_2^- was reduced to N_2O. The efficiency of NO_2^- removal was 72 ± 5%, and the efficiency of NO_2^- conversion to N_2O was 70 ± 5%. The maximum specific rate of N_2O production was 2.1 ± 0.4 mg of N_2O−N L^{-1} h^{-1}, and the efficiency of total reactive nitrogen removal efficiency was 80 ± 5% (Table 1).

Harvested cells isolated from the enrichment cultures grown in the decoupled mode contained inclusion granules visible by TEM (Figure S2). No such granules were observed in cells grown in the coupled mode.

To assess process stoichiometry, we computed carbon, nitrogen and electron balances for both the 48-h aerobic period (Table 2) and the 48-h anoxic period (Table 3). All triplicate measurements had relative errors <13%. During the 48-h aerobic period, CH_4 was used as a carbon and an electron source to produce non-P3HB biomass and intracellular P3HB. NH_4^+ was the sole nitrogen source for cell replication. During the 48-h anoxic period, the intracellular P3HB served as a carbon and an electron source for reduction of NO_2^- to N_2O and N_2. An electron balance (Table 3) indicates that P3HB oxidation provides reducing equivalents for partial denitrification of NO_2^- to N_2O.

Effect of O_2 and NO_2^- Concentrations on Methanotrophic N_2O Production. To evaluate the effect of NO_2^- and O_2 on N_2O production, we conducted triplicate serum bottle batch tests with P3HB-rich cells (removed after the 48-h aerobic step) amended with different levels of NO_2^- and O_2 (Figure 3). To obtain the maximum specific rate of N_2O production, we added acetylene (1%) to block reduction of N_2O to N_2.[5,25,26] Acetylene also inhibits methane monoxygenase[27] blocking use of CH_4 as the source of electrons for NO_2^- reduction but still allowing for oxidation of stored P3HB granules.

The maximum specific rate of N_2O production was 3.9 mg of N_2O g TSS^{-1} h^{-1} (Figure 3a). Using this value and observed

DOI: 10.1021/acs.est.5b03385
Environ. Sci. Technol. 2015, 49, 10969−10975

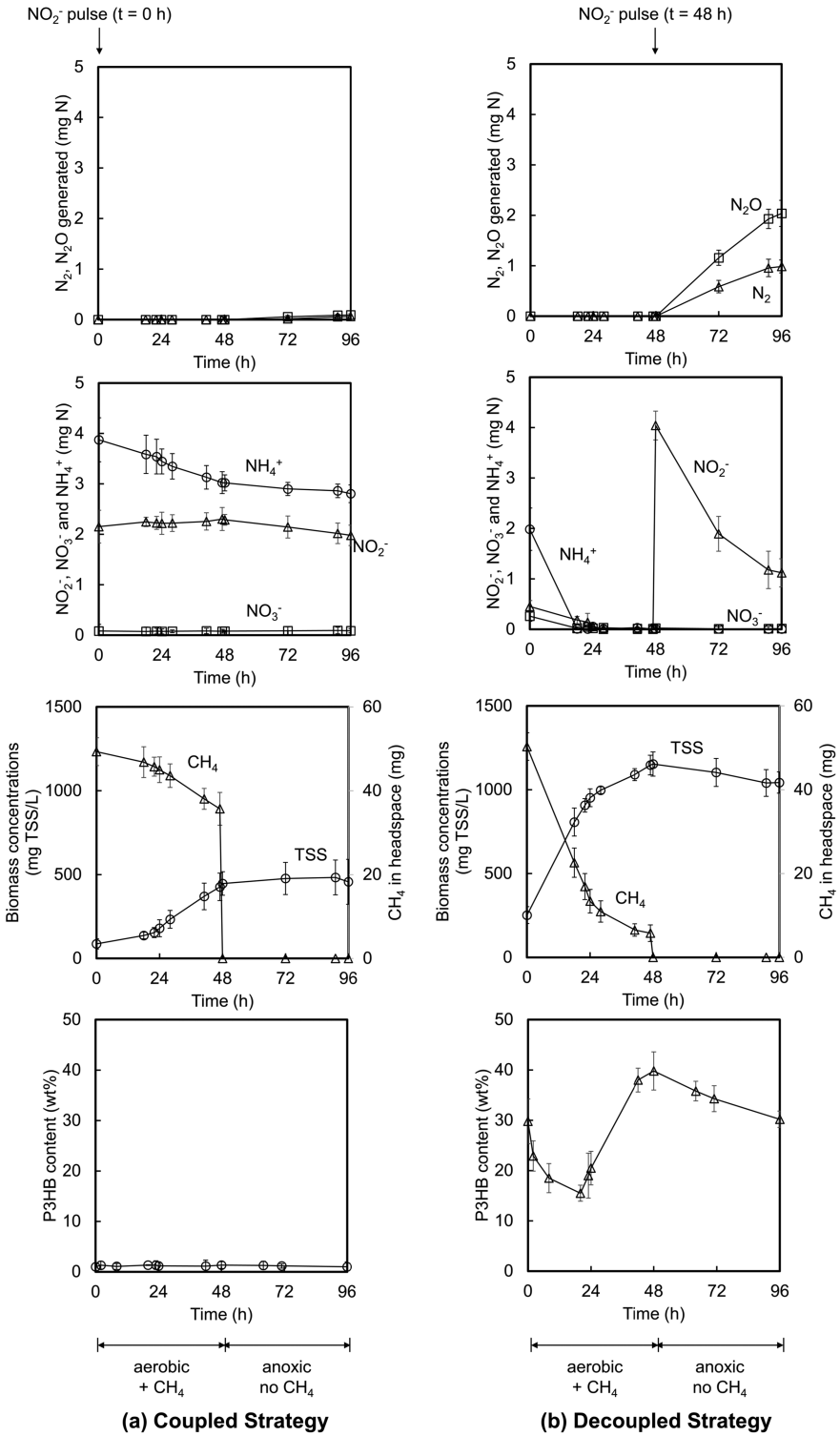

Figure 2. Various inorganic nitrogen concentrations, biomass concentrations (in mg of TSS/L), CH_4 in headspace and P3HB content (in wt %) for (a) coupled mode and (b) decoupled mode (cycle 24). Reported values are averages ± 1 standard deviation (N = 3).

initial rates at different levels of added NO_2^-, we quantified the kinetics of N_2O production, obtaining a half saturation coefficient of 39 ± 4 mg of NO_2−N/L. Reduction from NO_2^- to N_2O or N_2 requires several steps. At low NO_2^- concentration (<15 mg of NO_2−N/L), N_2 is the sole product. Reduction of NO_2^- to N_2O is likely slow relative to reduction of N_2O to N_2. At intermediate NO_2^- concentration (15−60 mg of NO_2−N/L), the rate of N_2O production increases rapidly. At high NO_2^- concentration (>60 mg of NO_2−N/L), the rate of production of both N_2O and N_2 stabilize as the supply of electron equivalents is limited by endogenous oxidation of P3HB under anoxic condition.

For the aerobic incubations, we added 80 mg of NO_2−N/L (a value about twice the half-saturation coefficient) and incubated P3HB-rich cells in the presence of different levels of added O_2. The maximum specific rate of N_2O production

DOI: 10.1021/acs.est.5b03385
Environ. Sci. Technol. 2015, 49, 10969−10975

Table 1. Reactor Performance Observed during a Typical Cycle[a]

	coupled mode	decoupled mode
NH_4^+ removal efficiency (%)	28 ± 5	99 ± 1
NO_2^- removal efficiency (%)	8 ± 3	72 ± 5
total reactive N removal efficiency (%)	19 ± 5	80 ± 5
efficiency of conversion from NO_2^- to N_2O (%)	6 ± 3	70 ± 5
max biomass concn (mg of TSS/L)	483 ± 105	1150 ± 72
max P3HB content (wt %)	4 ± 1	40 ± 3
obs max specific N_2O prod rate (mg of N_2O−N g VSS^{-1} h^{-1})	0.086 ± 0.010	2.1 ± 0.4
N_2O prod capacity (mg of N_2O−N L^{-1} h^{-1})	0.039 ± 0.009	2.3 ± 0.4

[a]Cycle 24. Reported values are averages ± 1 standard deviation (N = 3).

Table 2. Aerobic Growth and P3HB Production during a 48-h Aerobic Step (cycle 24): Mole Balance for Carbon, Nitrogen, And Electrons

	reactant moles				product moles		
reactants	carbon (C-mmol)	nitrogen (N-mmol)	electron (e-mmol)	products	carbon (C-mmol)	nitrogen (N-mmol)	electron (e-mmol)
CH_4	2.77 ± 0.12	0	22.2 ± 2.2	non-P3HB biomass ($C_5H_7O_2N$)	1.04 ± 0.23	0.21 ± 0.07	5.82 ± 0.87
O_2	0	0	0	P3HB biomass ($C_4H_6O_2$)	1.00 ± 0.12	0	3.74 ± 0.56
NH_4^+	0	0.14 ± 0.02	1.13 ± 0.22	CO_2	1.03 ± 0.22	0	0
NO_3^-	0	0.02 ± 0.01	0	H_2O	0	0	13.1 ± 2.2
NO_2^-	0	0.03 ± 0.01	0.06 ± 0.01				
sum	2.77 ± 0.12	0.19 ± 0.02	23.4 ± 2.2	sum	3.07 ± 0.34	0.21 ± 0.07	22.7 ± 2.4

Table 3. Anoxic Oxidation during a 48-h Anoxic Step (cycle 24): Mole Balance for Carbon, Nitrogen, and Electrons

	reactant moles				product moles		
reactants	carbon (C-mmol)	nitrogen (N-mmol)	electron (e-mmol)	products	carbon (C-mmol)	nitrogen (N-mmol)	electron (e-mmol)
P3HB biomass ($C_4H_6O_2$)	0.29 ± 0.05	0	1.08 ± 0.23	non-P3HB biomass ($C_5H_7O_2N$)	0.03 ± 0.01	0.01 ± 0.00	0.18 ± 0.02
O_2	0	0	0	CO_2	0.25 ± 0.02	0	0
NO_2^-	0	0.21 ± 0.02	0.42 ± 0.10	H_2O	0	0	0.25 ± 0.05
				N_2O	0	0.15 ± 0.02	0.58 ± 0.09
				N_2	0	0.07 ± 0.02	0.35 ± 0.09
sum	0.29 ± 0.05	0.21 ± 0.02	1.50 ± 0.25	sum	0.28 ± 0.02	0.23 ± 0.03	1.36 ± 0.16

decreased with increasing O_2 levels (Figure 3b) and stopped when the O_2 concentration in the headspace exceeded 30% by volume. Using a noncompetitive inhibition model to quantify the effects of added O_2, we obtained an inhibition coefficient of 2.9% by volume (1.3 mg/L dissolved O_2, assuming equilibrium with the gas phase). These results indicate a system that is highly sensitive to dissolved O_2 levels. Anoxic conditions favored N_2O production, but the presence of even small amounts of O_2 resulted in rerouting of electrons to O_2, the preferred electron acceptor.

■ DISCUSSION

Community structure and functional stability do not always correlate.[28] In this case, however, the type II methanotrophic enrichment cultures evaluated were stable in terms of both structure and function, consistently producing N_2O (note the small standard deviations for triplicate incubations in Figure 2) at elevated rates with minor changes in community structure (Figure 1). The mole balances for carbon, nitrogen, and electrons (Table 2 and Table 3) also indicate stable performance. A possible explanation is that NO_2^- pulsing imposed a strong selection pressure upon the community, limiting its variance. This has been observed in other systems. In a long-term study of sequencing batch reactor-fed phenol ± trichloroethylene (TCE), for example, a more stable community emerged in the TCE-stressed reactor, and this community was also functionally more stable for TCE degradation.[29]

Methanotrophic N_2O production is often regarded as minimal in comparison with denitrifying heterotrophs,[2] but this study suggests that in CH_4-rich environments, particularly those in which both NH_4^+ and NO_2^- are intermittently present, the contribution of methanotrophs should not be ignored. The N_2O conversion efficiency (~70%) and specific rate of N_2O production (2.1 mg of N_2O−N g VSS^{-1} h^{-1}) of methanotrophs is comparable to values reported for heterotrophs.[18,19]

Our results indicate that the decoupled N_2O production pattern previously observed with acetate-fed heterotrophic denitrifiers[19,30] is also observed in CH_4-fed enrichments. Decoupled addition of CH_4 and NO_2^- sustains both cell replication and P3HB accumulation. For cell replication, decoupled addition of CH_4 and NO_2^- is likely critical: for the coupled case, growth was severely inhibited (Figure 2; maximum specific growth rate decreased by a factor of 2.5). This is consistent with the observation that NO_2^- is a known inhibitor of CH_4 oxidation.[7,31,32]

Analysis of P3HB consumption and the N_2O production pattern (Figure 2) and electron balance during the anoxic period (Table 3) indicates that electrons from P3HB oxidation are used for reduction of NO_2^- to both N_2O and N_2 This is

DOI: 10.1021/acs.est.5b03385
Environ. Sci. Technol. 2015, 49, 10969−10975

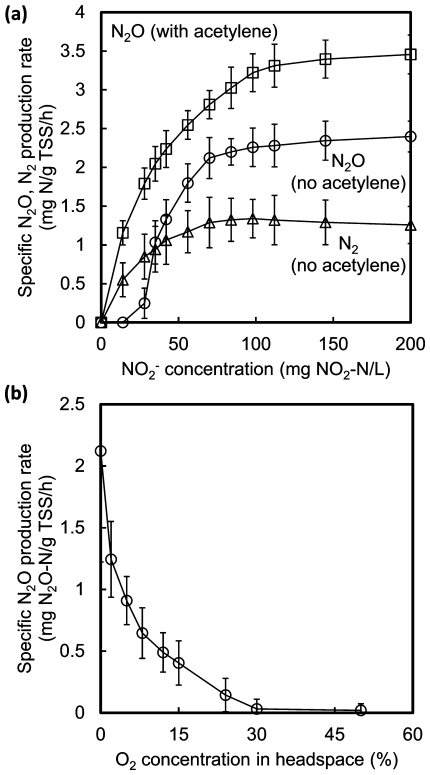

Figure 3. (a) Maximum specific rate of production of N_2O and N_2 as a function of added NO_2^- concentrations in batch anoxic incubations of P3HB-rich cells. (b) Maximum specific rate of N_2O production as a function of O_2 headspace concentrations in batch incubations of P3HB-rich cells. NO_2^- concentration was maintained at 80 mg of NO_2−N/L.

consistent with genomic analysis of the type II methanotroph *Methylocystis* sp. SC2 showing both a nitric oxide reductase (*norB*) and a complete N_2O reductase operon (*nosR*, *nosX*, *nosZ*).[33] In addition, *Methylocystis parvus* is known to possess a metabolic pathway for anaerobic degradation of intracellular P3HB granules.[34] The stoichiometry of these two reactions is summarized in eqs 1 and 2:

$$\frac{1}{18}C_4H_6O_2 + \frac{1}{2}NO_2^- + \frac{1}{2}H^+ \rightarrow \frac{2}{9}CO_2 + \frac{1}{4}N_2O + \frac{5}{12}H_2O \quad (1)$$

$$\frac{1}{18}C_4H_6O_2 + \frac{1}{3}NO_2^- + \frac{1}{3}H^+ \rightarrow \frac{2}{9}CO_2 + \frac{1}{6}N_2 + \frac{1}{3}H_2O \quad (2)$$

For partial denitrification eq 1, 0.68 g of P3HB/g of NO_2−N is required for NO_2^- reduction to N_2O. For complete denitrification to N_2 (eq 2), 1.0 g of P3HB/g of NO_2−N is required, a 50% increase. For the 70:30 ratio of N_2O/N_2, we would expect a P3HB demand of 0.78 g of P3HB/g of NO_2−N, but the observed P3HB consumption was 1.7 ± 0.1 g of P3HB/g of NO_2−N, suggesting an additional sink for P3HB. One possibility is P3HB fermentation under anaerobic conditions to low levels of soluble metabolites.[34]

Our results indicate that type II methanotrophs can mediate appreciable rates of N_2O production. A methanotrophic version of CANDO could potentially enable an operationally simple two-step process for removal of nitrogen from a high-NH_4^+ stream, such as anaerobic digester effluent. In step 1, ammonia-oxidizing bacteria convert NH_4^+ to NO_2^- via the SHARON process;[35] in step 2, methanotrophs convert NO_2^- to N_2O. Sustained delivery of biogas CH_4 with a limited supply of NH_4^+ could potentially enable growth of P3HB-accumulating methanotrophs, P3HB oxidation with coupled reduction of NO_2^- to N_2O, and stripping of N_2O for use as a co-oxidant of CH_4.[18]

■ ASSOCIATED CONTENT

Supporting Information

The Supporting Information is available free of charge on the ACS Publications website at DOI: 10.1021/acs.est.5b03385.

Detailed information on the methods for the bacterial community analysis, details on the difference between two feeding modes, a TEM image of the intracellular granules and a bacterial community structure of initial inoculum (PDF)

■ AUTHOR INFORMATION

Corresponding Author

*Phone: +1-650-723-9032; fax: +1-650-725-3164; e-mail: criddle@stanford.edu.

Notes

The authors declare no competing financial interest.

■ ACKNOWLEDGMENTS

This work was supported by the U.S. NSF Engineering Research Center: Re-Inventing the Nation's Urban Water Infrastructure (RENUWIt) under Award No. 1028968, unrestricted gifts from Chevron, and a Samsung Scholarship. We also thank the Stanford EM-1 Gas-Solution Analytical Center and Stanford Cell Sciences Imaging Facility for staff assistance, training, and access to instruments required for this research. We thank Dr. John J. Perrino for help on grid preparations and TEM visualization. The Jeol TEM 1400 was operated thanks to the NIH Grant SIG No. 1S10RR02678001. We also thank Prof. Perry L. McCarty for a helpful review of the manuscript.

■ REFERENCES

(1) Hanson, R. S.; Hanson, T. E. Methanotrophic bacteria. *Microbiol. Rev.* **1996**, *60* (2), 439−471.

(2) Yoshinari, T. Nitrite and nitrous oxide production by *Methylosinus trichosporium*. *Can. J. Microbiol.* **1985**, *31* (2), 139−144.

(3) Stein, L. Y.; Klotz, M. G. Nitrifying and denitrifying pathways of methanotrophic bacteria. *Biochem. Soc. Trans.* **2011**, *39* (6), 1826−1831.

(4) Kramer, M.; Bender, M. Consumption of NO by methanotrophic bacteria in pure culture and in soil. *FEMS Microbiol. Lett.* **1990**, *73*, 345−350.

(5) Ren, T.; Roy, R.; Knowles, R. Production and consumption of nitric oxide by three methanotrophic bacteria. *Appl. Environ. Microbiol.* **2000**, *66*, 3891−3897.

(6) Campbell, M. A.; Nyerges, G.; Kozlowski, J. A.; Poret-Peterson, A. T.; Stein, L. Y.; Klotz, M. G. Model of the molecular basis for hydroxylamine oxidation and nitrous oxide production in methanotrophic bacteria. *FEMS Microbiol. Lett.* **2011**, *322* (1), 82−89.

(7) Nyerges, G.; Han, S. K.; Stein, L. Y. Effects of ammonium and nitrite on growth and competitive fitness of cultivated methanotrophic bacteria. *Appl. Environ. Microbiol.* **2010**, *76* (16), 5648−5651.

(8) Hoefman, S.; van der Ha, D.; Boon, N.; Vandamme, P.; De Vos, P.; Heylen, K. Niche differentiation in nitrogen metabolism among

methanotrophs within an operational taxonomic unit. *BMC Microbiol.* **2014**, *14*, 83.
(9) Lee, S.-W.; Im, J.; Dispirito, A. A.; Bodrossy, L.; Barcelona, M. J.; Semrau, J. D. Effect of nutrient and selective inhibitor amendments on methane oxidation, nitrous oxide production, and key gene presence and expression in landfill cover soils: characterization of the role of methanotrophs, nitrifiers, and denitrifiers. *Appl. Microbiol. Biotechnol.* **2009**, *85* (2), 389−403.
(10) De Bont, J. A. M.; Mulder, E. G. Nitrogen Fixation and Co-oxidation of Ethylene by a Methane-utilizing Bacterium. *J. Gen. Microbiol.* **1974**, *83*, 113−121.
(11) Klotz, M. G.; Norton, J. M. Multiple copies of ammonia monooxygenase (amo) operons have evolved under biased AT/GC mutational pressure in ammonia-oxidizing autotrophic bacteria. *FEMS Microbiol. Lett.* **1998**, *168* (2), 303−311.
(12) Norton, J. M.; Alzerreca, J. J.; Suwa, Y.; Klotz, M. G. Diversity of ammonia monooxygenase operon in autotrophic ammonia-oxidizing bacteria. *Arch. Microbiol.* **2002**, *177* (2), 139−149.
(13) Sutka, R. L.; Ostrom, N. E.; Ostrom, P. H.; Gandhi, H.; Breznak, J. A. Nitrogen isotopomer site preference of N2O produced by *Nitrosomonas europaea* and *Methylococcus capsulatus* bath. *Rapid Commun. Mass Spectrom.* **2003**, *17* (7), 738−745.
(14) Mandernack, K. W.; Kinney, C. A.; Coleman, D.; Huang, Y. S.; Freeman, K. H.; Bogner, J. The biogeochemical controls of N2O production and emission in landfill cover soils: the role of methanotrophs in the nitrogen cycle. *Environ. Microbiol.* **2000**, *2* (3), 298−309.
(15) Lashof, D. A.; Ahuja, D. R. Relative contributions of greenhouse gas emissions to global warming. *Nature* **1990**, *344*, 529−531.
(16) Pfahl, U. J.; Ross, M. C.; Shepherd, J. E.; Pasamehmetoglu, K. O.; Unal, C. Flammability limits, ignition energy, and flame speeds in H2-CH4-NH3- N2O-O2-N2 mixtures. *Combust. Flame* **2000**, *123*, 140−158.
(17) Tsang, W.; Herron, J. T. Chemical Kinetic Data Base for Propellant Combustion I. Reactions Involving NO, NO2, HNO, HNO2, HCN and N2O. *J. Phys. Chem. Ref. Data* **1991**, *20*, 609.
(18) Scherson, Y. D.; Woo, S. G.; Criddle, C. S. Production of nitrous oxide from anaerobic digester centrate and its use as a co-oxidant of biogas to enhance energy recovery. *Environ. Sci. Technol.* **2014**, *48*, 5612−5619.
(19) Scherson, Y. D.; Wells, G. F.; Woo, S.-G.; Lee, J.; Park, J.; Cantwell, B. J.; Criddle, C. S. Nitrogen removal with energy recovery through N2O decomposition. *Energy Environ. Sci.* **2013**, *6*, 241.
(20) Rittmann, B. E.; McCarty, P. L. *Environmental Biotechnology: Principles and Applications*; McGraw-Hill: Boston, 2001.
(21) Zhao, S.; Fan, C.; Hu, X.; Chen, J.; Feng, H. The microbial production of polyhydroxybutyrate from methanol. *Appl. Biochem. Biotechnol.* **1993**, *39−40*, 191−199.
(22) Kassab, A. C.; Piskin, E.; Bilgic, S.; Denkbas, E. B.; Xu, K. Embolization with polyhydroxybutyrate (PHB) microspheres: in-vivo studies. *J. Bioact. Compat. Polym.* **1999**, *14*, 291−303.
(23) Martineau, C.; Mauffrey, F.; Villemur, R. Comparative analysis of denitrifying activities of *Hyphomicrobium nitrativorans*, *Hyphomicrobium denitrificans*, and *Hyphomicrobium zavarzinii*. *Appl. Environ. Microbiol.* **2015**, *81* (15), 5003−5014.
(24) Sperl, G. T.; Hoare, D. S. Denitrification with methanol: a selective enrichment for *Hyphomicrobium* species. *J. Bacteriol.* **1971**, *108* (2), 733−736.
(25) Balderston, W. L.; Sherr, B.; Payne, W. J. Blockage by acetylene of nitrous oxide reduction in *Pseudomonas perfectomarinus*. *Appl. Environ. Microbiol.* **1976**, *31* (4), 504−508.
(26) Yoshinari, T.; Knowles, R. Acetylene inhibition of nitrous oxide reduction by denitrifying bacteria. *Biochem. Biophys. Res. Commun.* **1976**, *69* (3), 705−710.
(27) Prior, S. D.; Dalton, H. Acetylene as a suicide substrate and active site probe for methane monooxygenase from *Methylococcus capsulatus* (Bath). *FEMS Microbiol. Lett.* **1985**, *29* (1), 105−109.
(28) Fernández, A.; Huang, S.; Seston, S.; Xing, J.; Hickey, R.; Criddle, C.; Tiedje, J. How stable is stable? Function versus community composition. *Appl. Environ. Microbiol.* **1999**, *65* (8), 3697−3704.
(29) Ayala-Del-Río, H. L.; Callister, S. J.; Criddle, C. S.; Tiedje, J. M. Correspondence between community structure and function during succession in phenol- and phenol-plus-trichloroethene-fed sequencing batch reactors. *Appl. Environ. Microbiol.* **2004**, *70* (8), 4950−4960.
(30) Qin, L.; Liu, Y.; Tay, J. H. Denitrification on poly-beta-hydroxybutyrate in microbial granular sludge sequencing batch reactor. *Water Res.* **2005**, *39* (8), 1503−1510.
(31) Dunfield, P.; Knowles, R. Kinetics of inhibition of methane oxidation by nitrate, nitrite, and ammonium in a Humisol. *Appl. Environ. Microbiol.* **1995**, *61* (8), 3129−3135.
(32) King, G. M.; Schnell, S. Ammonium and nitrite inhibition of methane oxidation by *Methylobacter albus* BG8 and *Methylosinus trichosporium* OB3b at low methane concentrations. *Appl. Environ. Microbiol.* **1994**, *60* (10), 3508−3513.
(33) Dam, B.; Dam, S.; Blom, J.; Liesack, W. Genome Analysis Coupled with Physiological Studies Reveals a Diverse Nitrogen Metabolism in *Methylocystis* sp. Strain SC2. *PLoS One* **2013**, *8* (10), 1−15.
(34) Vecherskaya, M.; Dijkema, C.; Saad, H. R.; Stams, A. J. M. Microaerobic and anaerobic metabolism of a *Methylocystis parvus* strain isolated from a denitrifying bioreactor. *Environ. Microbiol. Rep.* **2009**, *1* (5), 442−449.
(35) Hellinga, C.; Schellen, A. A. J. C.; Mulder, J. W.; Van Loosdrecht, M. C. M.; Heijnen, J. J. The SHARON process: An innovative method for nitrogen removal from ammonium-rich waste water. *Water Sci. Technol.* **1998**, *37* (9), 135−142.

DOI: 10.1021/acs.est.5b03385
Environ. Sci. Technol. 2015, 49, 10969−10975